

# Determination of metastable atom concentration by use of electrostatic probe technique

Dariusz Korzec<sup>a,\*</sup>, Mamunur Rashid Talukder<sup>b</sup>, Masashi Kando<sup>b</sup>

<sup>a</sup>Microstructure Research Center, University of Wuppertal, Fuhlrottstr. 10, 42119 Wuppertal, Germany

<sup>b</sup>Department of Electrical and Electronic Engineering, Shizuoka University, Shizuoka-Ken, Hamamatsu-Shi, Johoku 3-5-1, 432-8561, Japan

Received 19 February 2001; accepted 15 May 2001

## Abstract

A method for determination of the metastable atom concentration in high pressure ( $>100$  Torr) high density ( $>10^{12}\text{cm}^{-3}$ ) helium plasma from current–voltage characteristics of a single electrostatic probe is described. It is shown, that the flux of metastable atoms to the probe is controlled by ion sheath thickness and consequently by probe bias. The method for calculation of metastables concentration from the negative part of the current–voltage probe characteristics is proposed. The metastables concentrations measured in pulsed microwave discharge are in agreement with values calculated from the metastable balance equation. © 2001 Elsevier Science Ltd. All rights reserved.

**Keywords:** Plasma diagnostics; Electrostatic probe; Metastable helium; Atmospheric pressure discharge; Microwave discharge

## 1. Introduction

The role of metastable excited atoms, is well known and recognized for transfer and storing of energy [1]. Especially interesting are triplet ( $2^3\text{S}$ ) metastables of helium due to their extremely long radiative life time [2]. The application of metastable excited helium for gas chromatography [3], buffering energy in gas discharge lasers [4] or for high energy propulsion fuel [5] can be referred. An increasing interest is focused on applications for material synthesis and processing. The metastables are used as a source of chemical energy for low pressure pulsed plasma [6] or for reactive etching [7]. Recently their role for atmospheric pressure processing is stressed [8]. Especially important role play metastables for sustaining an atmospheric pressure glow (APG) [9], which can be used for surface treatment, [10] film deposition, [11] and film removal [12].

An electron ejection from metal surface by metastable atoms was first established for mercury metastable atoms incident on a nickel surface [13]. Oliphant [14] first observed electron ejection from metal surface by helium metastable atoms.

A lot of research effort was devoted to the characterization of metastable atoms and their interactions with metal surfaces at low pressure [15]. The influence of metastable

excited atoms on the probe characteristics is already long time known as a parasitic effect [16], making difficult the determination of ion concentrations at higher pressures [17]. Due to the Auger de-excitation of metastable excited atoms, a high secondary electron emission current can be observed. In this work, we propose the method for determination of metastables concentration in high pressure ( $>100$  Torr), high-density ( $>10^{12}\text{cm}^{-3}$ ) discharges by use of a probe technique. The change of electron emission current vs. negative polarization of the probe is observed in such discharges. This can be explained by influence of the ion sheath thickness on the metastables flux to the probe. Assuming, that no metastables are produced in the electron-free ion sheath, the diffusion determined metastables flux is increasing with decreasing ion sheath thickness (see Fig. 1). The proposed model allows to calculate the metastable concentration in the bulk plasma on the base of the negative branch of  $I$ – $V$  probe characteristics. The model for the case, when the ion sheath is thin or does not exist is also proposed, allowing the modeling of the saturation emission current.

## 2. Estimation of metastable concentration from balance equation

The concentration of the metastable excited atoms  $n_M$  can be calculated in a simplified way from the balance equation

\* Corresponding author. Tel.: +49-202-439-3798; fax +49-202-439-3010.

E-mail address: korzec@fmt.uni-wuppertal.de (D. Korzec).

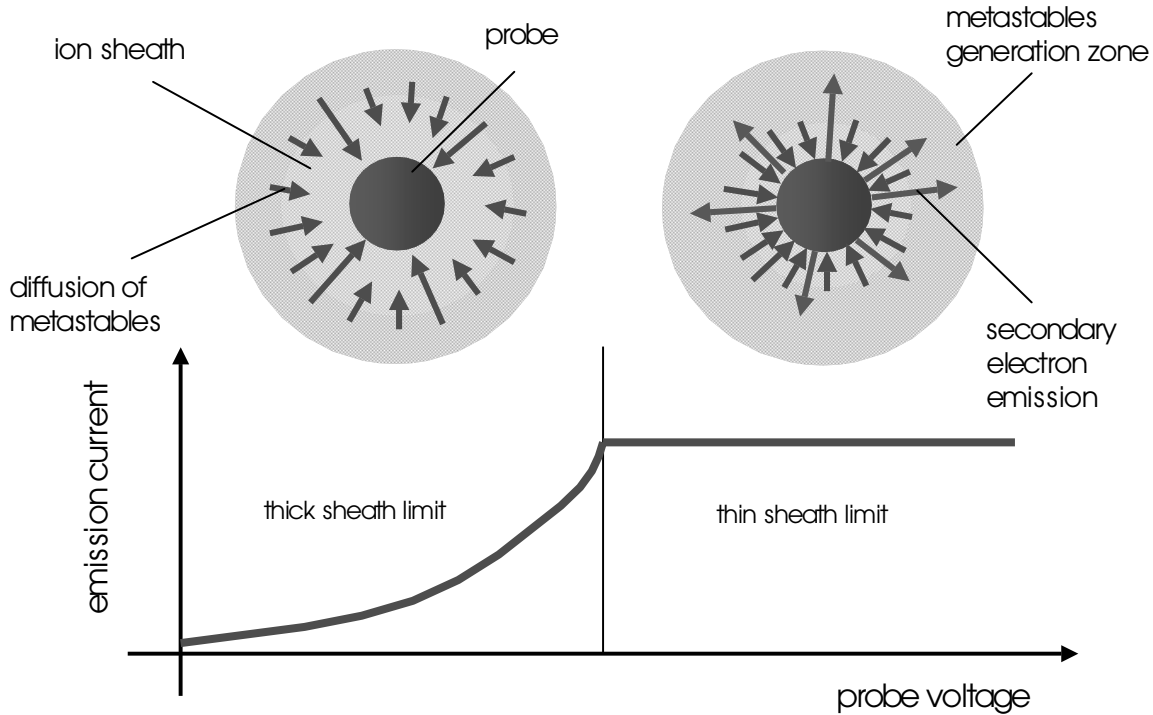


Fig. 1. Influence of the probe bias on the flux of metastable atoms to the probe surface.

for metastable excited atom concentration [4]:

$$\frac{\partial n_M}{\partial t} = D_M \nabla^2 n_M + S - P \quad (1)$$

$D_M$  is the diffusion coefficient and  $S$  and  $P$  are the volume creation and loss terms, respectively. Knowing the main production and destruction mechanisms and their rates, the steady state concentration of metastable excited atom can be found from Eq. (1). In next paragraphs such mechanisms will be briefly resumed.

2.1. Metastable excitation rate

For estimation of metastables production rate, only the electron impact excitation will be taken into account. The source term of Eq. (1) reduces to:

$$S = n_N n_e C_0^M \quad (2)$$

where  $n_e$  is the electron concentration and  $C_0^M$  is an electron temperature dependent rate coefficient for excitation of metastable state of helium from ground state.  $C_0^M$  can be calculated from the electron energy distribution function assumed as Maxwellian:

$$f(W) \frac{2}{\sqrt{\pi}} \left( \frac{e}{kT_e} \right) \sqrt{\frac{eW}{kT_e}} \exp\left(-\frac{eW}{kT_e}\right) \quad (3)$$

and from cross section for metastable excitation  $\sigma_M(W)$  shown vs. electron energy in Fig. 2 [18]. Using a linear approximation of the electron impact cross section for metastable excitation [2] close to the excitation threshold

$W_0$ , the production rate coefficient is given as:

$$C_0^M \int_{E_0}^{\infty} \sigma(W) \sqrt{\frac{2eW}{m_e}} f(W) dW = C_0 \sqrt{\frac{8e}{\pi m_e}} W_0 \sqrt{\frac{kT_e}{e}} \left( 1 + \frac{2kT_e}{eW_0} \right) \exp\left(-\frac{eW_0}{kT_e}\right) \quad (4)$$

$C_0$  is the constant referring to the slope of the linear approximation, given together with  $W_0$  in Table 1. For electron temperature corresponding to  $T_e = 4.4$  eV and triplet metastable state excitation energy  $W_0 = 19.82$  eV, these rate coefficient is  $C_0^M = 1.24 \times 10^{-16} \text{ m}^3 \text{ s}^{-1}$ .

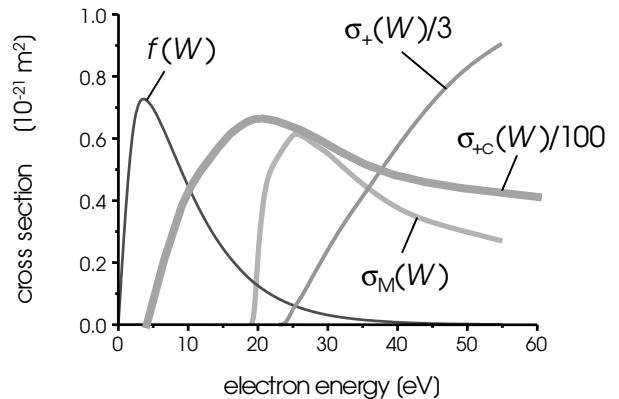


Fig. 2. Electron impact cross sections for ionization  $\sigma_+$ , cumulative ionization  $\sigma_{+c}$ , metastable excitation  $\sigma_M(E)$  and electron energy distribution function for electron temperature of 4.4 eV as a function of electron energy.

Table 1

Parameters used for linear approximation of the collision cross sections by Eq. (4) and the corresponding rate coefficients, collision frequencies and production rates for at typical experimental conditions ( $T = 973$  K,  $p = 700$  Torr), electron temperature of  $T_e = 4.4$  eV and electron concentration  $n_e = 3.5 \times 10^{20} \text{ m}^{-3}$ . For cumulative ionization calculation the metastables concentration of  $n_M = 0.76 \times 10^{22} \text{ m}^{-3}$  is taken

|                          | $W_0$ (eV) | $C_0$ ( $\text{m}^2/\text{eV}$ ) | Rate coefficient ( $\text{m}^3 \text{ s}^{-1}$ ) | Collision frequency ( $\text{s}^{-1}$ ) | Production rate ( $\text{m}^{-3} \text{ s}^{-1}$ ) |
|--------------------------|------------|----------------------------------|--|---|--|
| Direct impact ionization | 24.59      | $1.0 \times 10^{-22}$            | $C_0^+ = 1.8 \times 10^{-17}$                    | $1.22 \times 10^8$                      | $4.26 \times 10^{28}$                              |
| Cumulative ionization    | 4.77       | $1.7 \times 10^{-20}$            | $C_M^+ = 1.14 \times 10^{-13}$                   | $8.6 \times 10^8$                       | $3.0 \times 10^{29}$                               |
| Metastable excitation    | 19.82      | $2.8 \times 10^{-22}$            | $C_0^M = 1.24 \times 10^{-16}$                   | $8.6 \times 10^8$                       | $3.0 \times 10^{29}$                               |

The neutral particle concentration calculated according to formula:

$$n_N = \frac{P}{kT_N} \quad (5)$$

is  $n_N = 6.95 \times 10^{24} \text{ m}^{-3}$  at typical experimental conditions ( $T_N = 973$  K,  $p = 700$  Torr). With this value, the metastables generation frequency is  $0.86 \times 10^9 \text{ s}^{-1}$ . Taking the electron concentration of  $n_e = 3.5 \times 10^{20} \text{ m}^{-3}$  which is typical for our experimental conditions, the production rate is  $3.02 \times 10^{29} \text{ m}^{-3} \text{ s}^{-1}$ .

## 2.2. Volume losses of metastables

In general the metal walls of the plasma containment can be treated as an ideal sink for metastable atoms, but at high pressure and in sufficient distance from the plasma containment walls (in plasma bulk), the diffusion losses can be neglected comparing to volume losses. The three main metastables destruction processes [19] are considered for the loss term of Eq. (1). For all calculated examples the electron concentration  $n_e = 3.5 \times 10^{20} \text{ m}^{-3}$ , the electron temperature  $T_e = 4.4$  eV and the metastables concentration  $n_M = 0.79 \times 10^{22} \text{ m}^{-3}$  is taken.

The first volume loss mechanism takes into account only the de-excitation due to the three body collisions and is described by the expression

$$P = n_N^2 n_M K_M^0 \quad (6)$$

$K_M^0 = 2.5 \times 10^{-46} \text{ m}^6 \text{ s}^{-1}$  is quadratic destruction coefficient for  $2^3\text{S}$  metastables [20]. For neutral particles concentration of  $n = 6.95 \times 10^{24} \text{ m}^{-3}$  the destruction rate of this process is  $9.17 \times 10^{25} \text{ m}^{-3} \text{ s}^{-1}$ .

The second volume loss mechanism occurs due to ionization by the collision of metastables pairs [21] and is

described by destruction rate:

$$P = n_M^2 K_M^+ \quad (7)$$

$K_M^+$  is calculated from the cross section for this process of  $\sigma_M^+ = 10^{-18} \text{ m}^2$ . This value is obtained from expression:

$$K_M^+ = \sigma_M^+ v_M = \sigma_M^+ \sqrt{\frac{8kT_M}{\pi m_{\text{He}}}} \quad (8)$$

$m_{\text{He}}$  is the mass of helium atom.  $K_M^+ = 2.3 \times 10^{-15} \text{ m}^3 \text{ s}^{-1}$  for metastables temperature  $T_M = 973$  K. The corresponding destruction rate is  $1.33 \times 10^{29} \text{ m}^{-3} \text{ s}^{-1}$ .

The third loss mechanism is the destruction of metastables due to cumulative ionization. It can be described by destruction rate:

$$P = n_M n_e C_M^+ \quad (9)$$

The rate coefficient for cumulative ionization  $C_M^+$  can be calculated using Eq. (4) with linear approximation of the cross-section for cumulative ionization  $\sigma_{+C}(W)$  shown in Fig. 2 [2]. The parameter of the linear approximation for energy dependent cross-sections are shown in Table 1. With such obtained rate coefficient for cumulative ionization  $C_M^+ = 1.14 \times 10^{-13} \text{ m}^3 \text{ s}^{-1}$  the cumulative ionization rate of  $3.0 \times 10^{29} \text{ m}^{-3} \text{ s}^{-1}$  is obtained.

The described loss mechanisms are resumed in Table 2. The comparison of the three destruction rates calculated for typical discharge conditions shows, that the main loss mechanism in the plasma bulk is the cumulative ionization. This mechanism will be used for estimation of the metastables concentration.

## 2.3. Metastables concentration in plasma bulk

Taking into account the cumulative ionization as the dominating destruction process, the balance of metastables

Table 2

The three main destruction mechanisms of the metastable excited helium at atmospheric pressure in the bulk plasma. The electron temperature  $T_e = 4.4$  eV, neutral particle concentration  $n_N = 6.95 \times 10^{24} \text{ m}^{-3}$  and the metastables concentration  $n_M = 0.76 \times 10^{22} \text{ m}^{-3}$  are taken for calculations

|                         | Three-body de-excitation   | Binary metastable collision ionization  | Cumulative ionization  |
|-------------------------|--|---|--|
| Destruction mechanism   | $\text{He}(2^3\text{S}) + \text{He} + \text{He} \gamma \text{He}_2(2^3\text{S}_u^+) + \text{He}$ | $\text{He}(2^3\text{S}) + \text{He}(2^3\text{S}) \gamma \text{He}^+ + \text{He} + \text{e}$ | $\text{He}(2^3\text{S}) + \text{e} \gamma \text{He}^+ + 2\text{e}$ |
| Destruction rate        | $P = n_N^2 n_M K_M^0$  | $P = n_M^2 K_M^+$   | $P = n_M n_e C_M^+$  |
| Destruction coefficient | $K_M^0 = 2.5 \times 10^{-46} \text{ m}^6 \text{ s}^{-1}$   | $K_M^+ = 2.3 \times 10^{-15} \text{ m}^3 \text{ s}^{-1}$                                    | $C_M^+ = 1.14 \times 10^{-13} \text{ m}^3 \text{ s}^{-1}$          |
| Destruction rate        | $9.2 \times 10^{25} \text{ m}^{-3} \text{ s}^{-1}$   | $1.33 \times 10^{29} \text{ m}^{-3} \text{ s}^{-1}$   | $3.0 \times 10^{29} \text{ m}^{-3} \text{ s}^{-1}$                 |

in the plasma bulk can be written in simplified form as:

$$n_{M0}n_{e0}C_M^+ = n_N n_{e0} C_0^M \quad (10)$$

$n_{M0}$  and  $n_{e0}$  are metastables concentration and electron concentration in the plasma bulk, respectively.

The equilibrium metastable concentration is given as:

$$n_{M0} = n_N \frac{C_0^M}{C_M^+} \quad (11)$$

and for the example set of data is  $n_{M0} \approx 0.76 \times 10^{22} \text{ m}^{-3}$ .

The Eq. (11) can be used for estimation of the equilibrium metastable concentration only for plasmas with very high electron concentrations. It holds, for example, for high power microwave, ICP or jet discharges. In case of plasmas with low electron concentration (streamer discharges, atmospheric pressure glows, afterglows and remote plasmas) this condition is not fulfilled. Not only the cumulative ionization is losing its importance, but also the ionization by the binary metastables collisions get very small due to square dependence on metastable concentration strongly decreasing with decreasing electron concentration according to Eq. (2). In such cases the destruction due to the three body collisions is dominant. Consequently the Eq. (6) should be used for estimation of the equilibrium concentration of metastables, giving:

$$n_{M0} = \frac{n_{e0}}{n_N} \frac{C_0^M}{K_M^+} \quad (12)$$

### 3. Calculation of secondary electron emission current

In general, the emission of electrons from the probe surface can be caused by ion impact, electron impact, photo-emission or emission due to de-excitation of metastables. For high negative probe bias, emission due to electron impact is negligible. Since at high pressure the secondary electron emission current is on two orders of magnitude higher than the thermal ion current, especially when probe diameter is relatively large [22], the secondary electron current due to ion impact can also be disregarded.

Knowing the metastable flux to the probe and the secondary electron emission coefficient, the emission current due to the de-excitation of metastable atoms can be expressed as:

$$I_{em} = \gamma e S_p \Gamma_M \quad (13)$$

In following the calculation of the metastable particle flux to the probe will be presented. Then the method of determination of the effective secondary emission coefficient under consideration of electron recoil will be described.

#### 3.1. Metastables flux to the probe

For calculation of the metastable flux to the probe a

simple formula:

$$\Gamma_M = \frac{n_{M0}\bar{v}}{4} = n_{M0}\sqrt{\frac{kT_M}{2\pi m_{He}}} \quad (14)$$

was already proposed by Kagan and Perel [23], in which  $\bar{v}$  is the mean velocity of metastable atoms. With  $T_M = 973 \text{ K}$  and  $n_{M0} = 0.76 \times 10^{22} \text{ m}^{-3}$ , the estimated metastable flux is  $4.3 \times 10^{24} \text{ m}^{-2} \text{ s}^{-1}$ , which would result in a current 2 A emitted from the probe with surface area of  $3 \times 10^{-6} \text{ m}^2$ . This value is on two orders of magnitude higher, than the negative currents really occurring in the probe characteristics, because Eq. (14) holds only for the ion sheath thickness smaller than the free path for metastable particles. Assuming the plasma sheath thickness of  $10 \text{ }\mu\text{m}$ , the pressure limit for applicability of Eq. (14) in helium is about 12 Torr.

For much higher pressures a continuum model have to be used. The flux of metastables can be obtained from Eq. (1), for the vicinity of the probe surface. Due to a high concentration gradient, the diffusion term cannot be neglected. In general this problem can be solved only numerically, but we propose two one-dimensional solutions by use of: (i) the thin ion sheath approximation with constant electron concentration in the entire probe vicinity and (ii) the thick sheath approximation with zero electron concentration in the ion sheath and constant electron concentration in the plasma bulk. In both cases the metastables concentration at the probe surface can be regarded as zero, due to very high probability of metastables de-excitation.

#### 3.2. Thin ion sheath approximation

If the ion sheath is thin, the ion sheath edge can be treated as an equivalent of the probe surface, it means as a place of zero metastables concentration. The metastables concentration profile along y-axis can be obtained from Eq. (1) written for static, one dimensional case. Using the metastables production as described by Eq. (2) and destruction as given by Eq. (9), a differential equation:

$$D_M \frac{\partial n_M(y)}{\partial y} + n_N n_{e0} C_0^+ - n_M(y) n_{e0} C_M^+ = 0 \quad (15)$$

is obtained. For boundary conditions:

$$n_M(0) = 0 \quad n_M(\infty) = n_{M0} \quad (16)$$

the solution of Eq. (15) is given [24] as:

$$n_M(y) = n_{M0} \left[ \sinh\left(\frac{y}{\delta_0}\right) - 2 \sinh^2\left(\frac{y}{2\delta_0}\right) \right] \quad (17)$$

where

$$\delta_0 = \sqrt{\frac{D_M}{n_{e0} C_M^+}} \quad (18)$$

For  $n_{M0} = 0.76 \times 10^{22} \text{ m}^{-3}$ , the metastables diffusion constant  $D_M = 4.19 \times 10^{-4} \text{ m}^2 \text{ s}^{-1}$  and the coefficient of cumulative ionization of  $1.14 \times 10^{-13} \text{ m}^{-3} \text{ s}^{-1}$ , the

characteristic length of the metastables depletion zone  $\delta_0 = 3.24 \mu\text{m}$  is obtained.

Using the first derivative of the metastables concentration for  $y = 0$ , the metastables flux can be obtained:

$$\Gamma_M = -n_{M0}\sqrt{D_M n_{e0} C_M^+} \quad (19)$$

Combining the Eqs. (13) and (19) the metastables induced secondary electron emission current can be expressed as:

$$I_{em} = e\gamma S_p \Gamma_M = -e\gamma S_p n_{M0} \sqrt{D_M C_M^+ n_{e0}} \quad (20)$$

The thin ion sheath approximation can be applied, when the ion sheath thickness is much smaller than  $2\delta_0$ . It corresponds conditions at the probe surface, when the normalized probe potential is slightly negative or positive.

### 3.3. Thick ion sheath approximation

The assumption, that the ion sheath is electron-free, means that no metastables production due to electron impact and no losses due to stepwise ionization in this zone occur. The metastables concentration profile within the ion sheath can be obtained from Eq. (1) written under neglect of volume production and destruction as:

$$D_M \frac{\partial n_M(y)}{\partial y} = 0 \quad (21)$$

For boundary conditions:

$$n_M = (0) = 0 \quad n_M(\delta_{sh}) = n_{M0} \quad (22)$$

the solution of Eq. (21) is given as:

$$n_M(y) = n_{M0} D_M \frac{y}{\delta_{sh}} \quad (23)$$

$\delta_{sh}$  is the ion sheath thickness.

The metastables flux can be obtained using the first derivative of the metastables concentration distribution described by Eq. (23) for  $y = 0$ :

$$\Gamma_M = -D_M \frac{n_{M0}}{\delta_{sh}} \quad (24)$$

Substituting the metastables flux in Eq. (13) by Eq. (24), the expression for metastables induced electron emission current is obtained:

$$I_{em} = -\gamma e S_p D_M \frac{n_{M0}}{\delta_{sh}} \quad (25)$$

The thick ion sheath approximation is applicable, when: (i) the ion sheath thickness is larger than  $\delta_0$ . It holds for strong negative polarization of the probe, (ii) the metastables concentration at the ion sheath edge can be regarded as equal to the concentration in the plasma bulk  $n_{M0}$ . This requirement means that depletion of metastables at the sheath edge due to the metastables flux through the sheath is small, which is fulfilled for high electron concentration and consequently high production rate of metastables.

### 3.4. Diffusion constant for metastables

The diffusion constant of metastable excited helium atoms (triplet) through helium gas is a function of total particle concentration and of temperature [25] and can be expressed by approximation formula:

$$D_M = D_0 \left( \frac{p_0}{p} \right) \left( \frac{T_N}{T_0} \right)^\eta \quad (26)$$

where  $p_0$  is the pressure of 760 Torr,  $T_0$  the temperature of 273 K,  $D_0 = 5.59 \times 10^{-5} \text{ m}^2 \text{ s}^{-1}$  the metastables diffusion constant recalculated for  $T_0$  and  $p_0$  from Ref. [26], and  $\eta = 1.52$  is determined as a least square fit to the available quantum-mechanic calculations for temperature dependence of the diffusion constant [27]. For typical experimental conditions: pressure of 700 Torr and gas temperature of 973 K, the diffusion constant calculated from Eq. (14) is  $D_M = 4.19 \times 10^{-4} \text{ m}^2 \text{ s}^{-1}$ .

### 3.5. Ion sheath thickness

The thickness of the ion sheath may be evaluated by means of a simple model, which includes the one-dimensional Poisson equation written under the assumption of a negligible electron concentration within the sheath:

$$\frac{\partial^2 \Phi}{\partial y^2} = -\frac{en_+}{\epsilon_0} \quad (27)$$

The zero of the potential  $\Phi$  is chosen at the edge of the ion sheath. Hence the ion sheath thickness under our experimental conditions is on two orders of magnitude smaller than the probe radius, linear coordinates can be used. The continuity equation for ions is given as:

$$n_+ v_+ = -\Gamma_+ \quad (28)$$

where  $v_+$  is the local ion velocity in the direction towards the surface. The equation relating  $v_+$  to field gradient in the case of collision-dominated ion layer reads

$$v_+ = \mu_+ \frac{\partial \Phi}{\partial y} \quad (29)$$

$\mu_+$  denotes the ion mobility, which will be assumed to be constant across the ion sheath for simplicity.

Solving the above equations with the boundary condition of zero field at the edge of the ion sheath, one finds the following expressions for the ion sheath thickness [28]:

$$\delta_{sh} = \sqrt[3]{\frac{9\epsilon_0 \mu_+ V_{sh}^2}{8e|\Gamma_+|}} = \sqrt[3]{\frac{9\epsilon_0 \mu_+ S_p V_{sh}^2}{8|I_+|}} \quad (30)$$

where  $S_p$  is the probe surface area and  $V_{sh}$ , is the voltage across the sheath.

Considering our typical plasma parameter, the change of probe voltage from 30 to 60 V results in ion current increase of less than 5% [29]. Taking into account the coefficient of

ambipolar diffusion for case  $T_e \gg T_+$  :

$$D_a = \frac{kT_e}{e} \mu_+ \quad (31)$$

the ion current flowing to the probe is given as [28]:

$$I_+ = eS_p \Gamma_+ = -eS_p D_a \frac{n_{e0}}{\delta} = -S_p \mu_+ \frac{kT_e n_{e0}}{\delta} \quad (32)$$

where  $\delta$  is the specific scale length which is the lowest of the length scales: (i) probe radius  $R_p$ , (ii) Péclet number, playing role only for fast moving plasmas and (iii) free path for electron impact ionization  $\lambda_{e+}$ .

The free path for electron impact ionization  $\lambda_{e+}$  can be estimated by use of following expression:

$$\lambda_{e+} = \frac{1}{n_N \sigma_{e+}(W)} \quad (33)$$

and is in our case about 40  $\mu\text{m}$  — much less than the probe radius. Consequently Eq. (32) can be written as:

$$I_+ = -S_p \mu_+ \frac{kT_e n_e}{\lambda_{e+}} \quad (34)$$

Taking into account the Eq. (34) in Eq. (30), the ion sheath thickness can be expressed as:

$$\delta_{\text{sh}} = \frac{3}{2} \sqrt[3]{\frac{1}{3} \lambda_{e+} \lambda_D^2 \varphi_p^2} \quad (35)$$

where

$$\lambda_D = \sqrt{\frac{\epsilon_0 kT_e}{n_e e^2}} \quad (36)$$

is the Debye length and

$$\varphi_p = \frac{e(\Phi_s - V_p)}{kT_e} \quad (37)$$

is the normalized probe potential. For typical discharge conditions and normalized potential of 5, the plasma sheath thickness is 9.2  $\mu\text{m}$ .

Introducing the diffusion constant calculated according to Eq. (26) and the ion sheath thickness described by Eq. (35) in Eq. (24) allows the calculation of the metastable atom flux to the probe.

### 3.6. Effective secondary emission coefficient

Hagstrum [30] found, that on an atomically clean tungsten surface, slow rare-gas metastable atoms and ions should exhibit the same electron yield. The reason for this is, that metastable atoms are ionized by the tunneling of the excited electron to the metal. Both incident ions and metastable atoms are ions when they eject electrons.

The determination of an effective secondary electron emission coefficient  $\gamma$  at high pressure requires taking into account the backscattering of electrons emitted from the probe surface. The typical value of secondary electron emission coefficient for vacuum  $\gamma_0$  [31] under our experimental

condition is 0.29. It must be multiplied by an  $E/p$ -dependent factor [32] for arbitrary pressure.  $\gamma(E/p)/\gamma_0$  is increasing with increasing negative biasing of the probe. The mean value of the electric field in the ion sheath can be expressed as:

$$E_{\text{sh}} = \frac{2}{3} \frac{V_{\text{sh}}}{\delta_{\text{sh}}} = \frac{4}{9} \frac{kT_e}{e} \sqrt[3]{\frac{3|\varphi_p|}{\lambda_{e+} \lambda_D^2}} \quad (38)$$

The ratio of effective secondary electron emission coefficient  $\gamma(\chi)$  to secondary electron emission coefficient in vacuum  $\gamma_0$  is a function of the reduced electric field  $\chi = E/p$  and is given for helium as [32]:

$$\frac{\gamma(\chi)}{\gamma_0} = \frac{1}{\alpha w_{\text{max}}} \left( \frac{\chi}{\chi_1} \right)^{1/3} \ln \left[ \frac{1 + \psi(w_{\text{max}}) \frac{\chi_1}{\chi} + \alpha w_{\text{max}} \left( \frac{\chi_1}{\chi} \right)^{1/3}}{1 + \psi(w_{\text{max}}) \left( \frac{\chi_1}{\chi} \right)} \right] \quad (39)$$

The function  $\psi(w_{\text{max}})$ , taking into account the energy distribution of the emitted secondary electrons, can be approximated by:

$$\psi(w_{\text{max}}) = \frac{a}{w_{\text{max}}} \left[ -\frac{(1+b)}{b^3} \ln(1+bw_{\text{max}}) + \frac{(b+1)}{b^2} w_{\text{max}} - \frac{1}{2b} w_{\text{max}}^2 \right] \quad (40)$$

where

$$w_{\text{max}} = \frac{W_{\text{max}}}{W_{\text{ex}}} \quad (41)$$

$W_{\text{max}}$  is the maximum energy of emitted electrons and depends on the gas-surface material combination. For helium and tungsten  $W_{\text{max}} = 14$  eV [33].  $W_{\text{ex}}$  is the excitation energy of interest. For our estimation we have taken  $W_{\text{ex}} = 19.82$  eV.

The gas dependent constants  $a$ ,  $b$  and  $\alpha$  for helium are 7.53, 8.3 and 1.27, respectively. Here we denote the characteristic electric field  $\chi_1$  as:

$$\chi_1 = \frac{E_{\text{ex}}}{p} = \frac{W_{\text{ex}}}{e \lambda_e k T_N n_N} = \frac{W_{\text{ex}}}{e} \frac{\sigma_e(W_{\text{ex}})}{k T_N} \quad (42)$$

Elastic collision cross section for electron in helium [34] can be described in energy range from 3.4 to 28 eV by use of a fitting formula:

$$\sigma_e(W) = \left[ 1.3 + 4.9 \exp\left(-\frac{W}{14.8 \text{ eV}}\right) \right] \times 10^{-20} \text{ m}^2 \quad (43)$$

where  $W$  is the electron energy in eV. The accuracy of this formula is better than 2%, with an exception of the small zone from 18.4 to 20 eV where maximum error is 10%.

Using Eq. (43) for energy of metastable excitation (triplet) of 19.82 eV, cross section of  $\sigma_e = 2.58 \times$

$10^{-20} \text{ m}^2$  is obtained. With this value, normalized probe potential of 5 and electron temperature of 4.4 eV, after calculation of Eqs. (39)–(42), the ratio of effective secondary electron emission coefficient to secondary electron emission coefficient in vacuum is 0.49. The change of normalized probe potential from 5 to 10 causes according to Eq. (39) the increase of the effective secondary electron emission coefficient changes from 0.141 to 0.153, which means a change on about 8%.

In low-pressure experiments nitrogen and air contamination of the tungsten surface has been observed to reduce the electron yield of helium metastable atoms [35]. This reduction is approximately 45% for nitrogen and 80% for air. We expect, that no detrimental effect occurs in helium at atmospheric pressure, because the probe surface is not corroding and is permanently bombarded and cleaned by high flux of helium atoms and ions, so that an effective secondary electron emission coefficient of 0.15 will be considered as a constant for determination of metastables concentration from the measured data.

#### 4. Determination of metastable concentration from probe characteristics

In previous chapter the current of electrons emitted from the probe was calculated from the metastable atom concentration. The aim of the following derivation is just opposite: from known current–voltage characteristics the metastable atom concentration should be determined.

In general, the current flowing to the probe in an electro-positive plasma consists of the collected electron current  $I_e$ , collected positive ion current  $I_+$  and emitted electron current  $I_{em}$ :

$$I_p = I_e - I_+ - I_{em} \tag{44}$$

The collected electron current can be neglected for high negative probe voltage. The number of collisions of ion with neutral particles on its way from the plasma bulk to the probe surface increases proportional to pressure. The collisions of ions cause that the ion flux reaching the probe surface is much smaller than the random thermal flux. Considering our typical experimental conditions at atmospheric pressure, ion current at moderate negative probe polarization is in range from  $\mu\text{A}$  to tens of  $\mu\text{A}$ . It is on two orders of magnitude less than the typically measured electron emission current and can be neglected for the determination of metastables concentration.

##### 4.1. Fitting of the emission current

For strong negative polarized probe, when the condition of thick sheath approximation are fulfilled, the emission current can be obtained from Eq. (25) with sheath thickness

substituted by Eq. (35) and is given as:

$$I_{em} = \frac{2}{3} \frac{\gamma e S_p D_M}{\sqrt[3]{\frac{1}{3} \lambda_e + \lambda_D^2}} n_{M0} |\varphi_p|^{-2/3} \tag{45}$$

From Eq. (45) under consideration of Eq. (37) a simple formula for fitting of the negative branch of probe IV-characteristics can be obtained:

$$I_p = -I_{em} = -P_0 (\Phi_s - V_p)^{-2/3} \tag{46}$$

where  $\Phi_s$  is plasma space potential.  $P_0$  is a fitting parameter, from which  $n_{M0}$  can be calculated. Comparison of the  $I_{em}$  from Eqs. (45) and (46) gives:

$$n_{M0} = \frac{3}{2} \frac{P_0}{\gamma e S_p D_M} \left( \frac{q}{kT_e} \right)^{2/3} \sqrt[3]{\frac{1}{3} \lambda_e + \lambda_D^2} \tag{47}$$

##### 4.2. Saturation region of emission current

According to the predictions of the thin sheath model, the emission current expressed by Eq. (20) is not directly dependent on the probe potential and can be interpreted as a saturation value  $I_{em0}$  of emission current, achieved when probe gets strong positive. The emission current characteristic is explained in Fig. 1. The minimum of the measured I–V probe characteristics can be used as an approximation for  $I_{em0}$ . Subtracting this value from the probe current, the collected electron current is obtained. In Fig. 3 a typical current voltage probe characteristics at 700 Torr and the corresponding modeled lines are shown.

Using the saturation emission current for calculation of metastables concentration on the base of thin sheath model looks to be an attractive alternative to the thick sheath model. The deficiency of this approach is, that the effective secondary emission coefficient  $\gamma$  cannot be determined accurately, because the field strength and real sheath thickness are unknown under conditions of the thin film approximation. The agreement between the experimentally

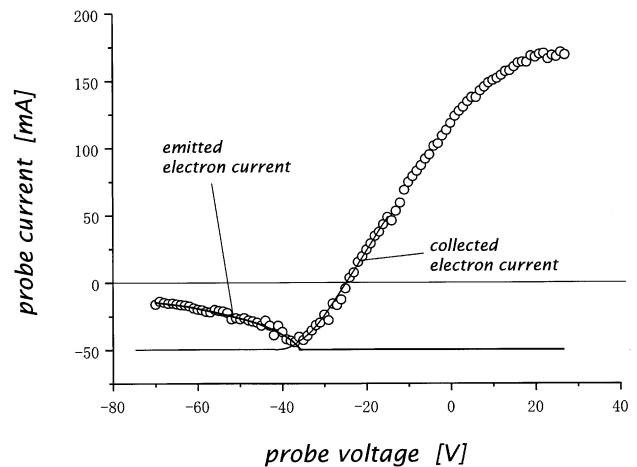


Fig. 3. The typical probe current–voltage characteristics collected at 700 Torr and curves explaining the collected and emitted electron current.

determined saturation current and predictions of Eq. (35) is possible, when  $\gamma$  is about 0.05. This is three times less than  $\gamma$  for high negative polarization.

Hence the applied model for the effective secondary emission coefficient is working only for strong negative probe polarization, we propose the fitting of I–V characteristics as a technique for determination of metastables concentration.

4.3. Fitting of collected electron current

The metastable concentration can be calculated from Eq. (47), only when both electron temperature and electron concentration needed for calculation of the Debye length are known. They can be obtained from the positive branch of the I–V probe characteristics. For this purpose the numerical analysis based on simultaneous solution of Poisson’s equation and continuity equations for spherical probe in continuum plasma [29] is used. The results of this study are available as a set of curves, representing the normalized electron current vs. normalized probe potential, for discrete values of Debye number, as shown in Fig. 4. The Debye number is defined as the ratio of probe radius to Debye length. To make this results usable for plasma diagnostics and hence for arbitrary Debye number, the approximation function for normalized electron current can be used:

$$\frac{I_e}{I_{e0}} = \frac{\exp\left(\frac{-\varphi_p}{A}\right)}{0.87 + 0.13 \exp\left(\frac{\varphi_p}{B}\right)} \tag{48}$$

where  $A$  and  $B$  are parameters dependent on the Debye number as follows:

$$A = 23.65 - 5.78 \log\left(\frac{R_p}{\lambda_D}\right) \tag{49}$$

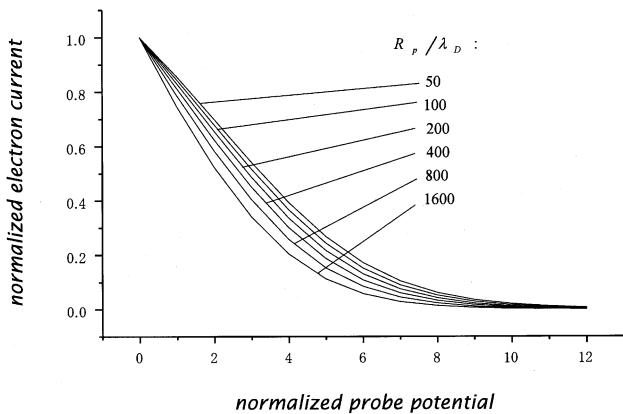


Fig. 4. The normalized electron current calculated by Cohen [29] for different values of Debye number as a function of the normalized probe potential. The thermal electron current  $I_{e0}$  used for normalization is defined by Eq. (51).

and

$$B = 2.19 - 0.154 \log\left(\frac{R_p}{\lambda_D}\right) \tag{50}$$

The Eq. (48) can be used under assumption, that the ion temperature is much smaller than the electron temperature, what is holding in pulsed microwave plasmas [8]. The thermal electron current  $I_{e0}$  is defined as:

$$I_{e0} = eS_p \frac{n_e v_{e,th}}{4} \left(\frac{4}{3} \frac{\lambda_e}{R_p}\right) \tag{51}$$

where the thermal speed of electrons is given as:

$$v_{e,th} = \sqrt{\frac{8kT_e}{\pi m_e}} \tag{52}$$

Assuming a constant value of the electron emission current  $I_{em0}$  (see Fig. 3) in the voltage range, in which the collected electron current is nonzero, the measured values of the probe current are least square fitted by:

$$I_e = I_{e0} \frac{\exp\left(\frac{-\varphi_p}{A}\right)}{0.87 + 0.13 \exp\left(\frac{\varphi_p}{B}\right)} - I_{em0} \tag{53}$$

From thermal electron current and Debye number used as fitting parameter, the electron temperature and electron concentration can be calculated. The example of such fitting is shown in Fig. 5. The plasma parameters displayed in Tables 3 and 4 are obtained this way. The detailed description of the iterative procedure for determination of electron temperature and electron concentration from measured current–voltage characteristics of a spherical probe is published elsewhere [36].

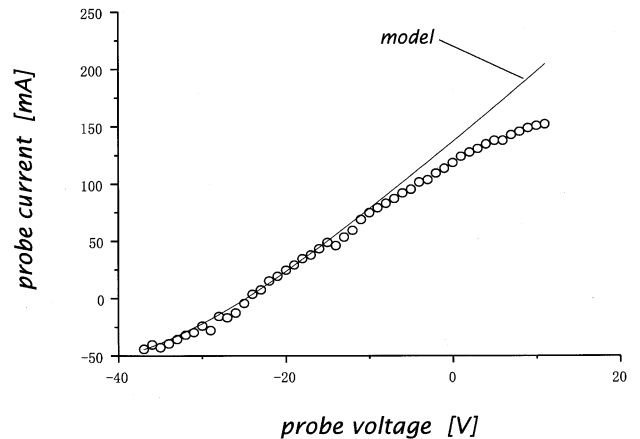


Fig. 5. Example of a fitting function according to Eq. (53) for determination of electron concentration and electron temperature from probe characteristics shown in Fig. 3.

Table 3

The plasma parameters, fitting parameters and the metastables concentrations calculated from  $P_0$  according to Eq. (47) for three probe characteristics shown in Fig. 8

| Curve-no                              | 1     | 2     | 3     |
|---------------------------------------|-------|-------|-------|
| $n_e$ ( $10^{20} \text{ m}^{-3}$ )    | 3.01  | 3.31  | 3.53  |
| $T_e$ (eV)                            | 4.5   | 3.8   | 4.2   |
| $\lambda_D$ ( $\mu\text{m}$ )         | 0.91  | 0.80  | 0.81  |
| $\Phi_s$ (V)                          | -7.9  | -7.9  | -7.9  |
| $P_0$ ( $\text{AV}^{2/3}$ )           | 0.158 | 0.180 | 0.203 |
| $n_{M0}$ ( $10^{22} \text{ m}^{-3}$ ) | 0.64  | 0.75  | 0.80  |

Table 4

The plasma parameters, emission current fitting parameters and the metastables concentrations calculated from  $P_0$  according to Eq. (47) for probe characteristics shown in Fig. 9

| Position                              | Edge  | Axis  |
|---------------------------------------|-------|-------|
| $n_e$ ( $10^{20} \text{ m}^{-3}$ )    | 3.22  | 1.09  |
| $T_e$ (eV)                            | 4.38  | 2.82  |
| $\lambda_D$ ( $\mu\text{m}$ )         | 0.87  | 1.20  |
| $\Phi_s$ (V)                          | -8    | -8    |
| $P_0$ ( $\text{AV}^{2/3}$ )           | 0.167 | 0.098 |
| $n_{M0}$ ( $10^{22} \text{ m}^{-3}$ ) | 0.67  | 0.68  |

## 5. Experiment

### 5.1. Setup

The detailed description of the setup is published elsewhere [8]. A 2.45 GHz pulsed magnetron with a 120 Hz repetition frequency is used. Sinus-shaped power pulses with duration of 2.3 ms are applied in each power pulse cycle, with maximum power of up to 1.5 kW. The discharge chamber consists of a rectangular WR-430 waveguide (see

Fig. 6a) closed on both ends with Pyrex glass plates. Two cylindrical tungsten pipes, with inner and outer diameters 4 and 6 mm, respectively, are inserted vertically at the center of each H plane of the waveguide, as shown in Fig. 6b. The spacing between the stub edges is 10 mm. A tungsten wire with diameter of 0.8 mm and length of 1 mm is inserted into the discharge zone through one of tungsten pipes. Its tip is positioned in the center or at the edge of the discharge, in the middle of space between the tube ends (see Fig. 7).

For the evaluation of probe characteristics an equivalent probe radius  $R_p$  is used. It is defined as a radius of a sphere, which has a surface area  $S_p$  identical to the surface of the real probe, as dimensioned in Fig. 7. It means for  $S_p = 3 \text{ mm}^2$  the equivalent radius  $R_p = 0.5 \text{ mm}$ . The data points of the current–voltage characteristics are collected during many power cycles with synchronized time from the start of the power pulse.

### 5.2. Determination of metastables concentration

In Fig. 8 the negative branches of I–V characteristics measured at 700 Torr in helium are shown. They are collected for three time points during increasing part of the power pulse: 1.0, 1.3 and 1.9 ms from the pulse start for curves 3, 2 and 1, respectively. The time dependent power decrease is explaining the decrease of the electron concentration. The Eq. (48) was applied for fitting of these curves and for determination of the metastables concentration in the range of voltages at which current is decreasing vs. negative probe voltage. The fitting parameters and the metastables concentrations calculated from  $P_0$  are displayed in Table 3. The metastables concentrations correlate well with values calculated from Eq. (11).

In the investigated plasma, about 0.2% of the total neutral

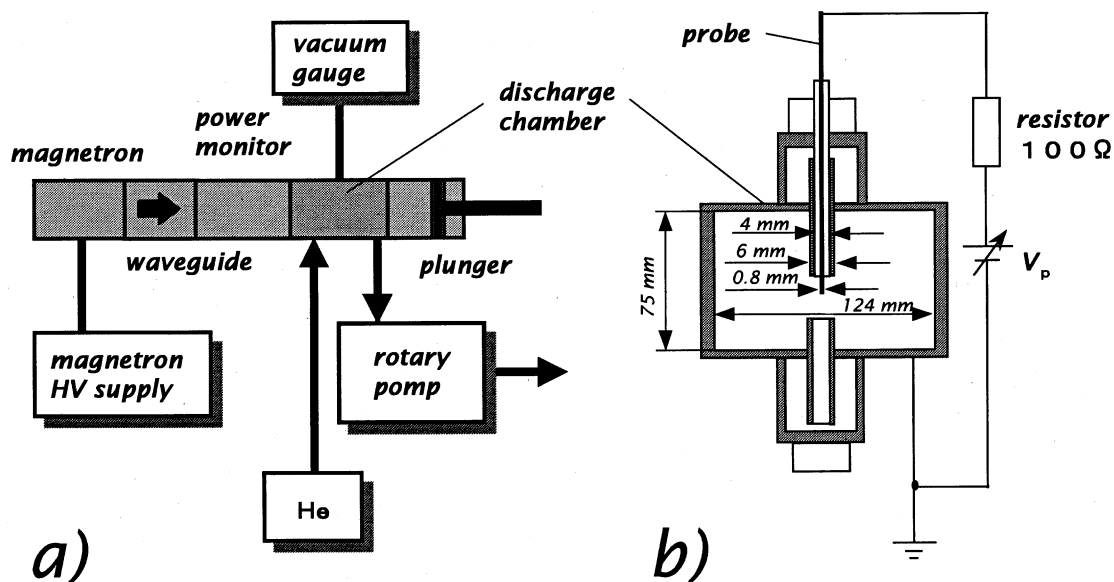


Fig. 6. (a) The microwave power supply system and (b) the structure of the discharge chamber of the experimental apparatus.

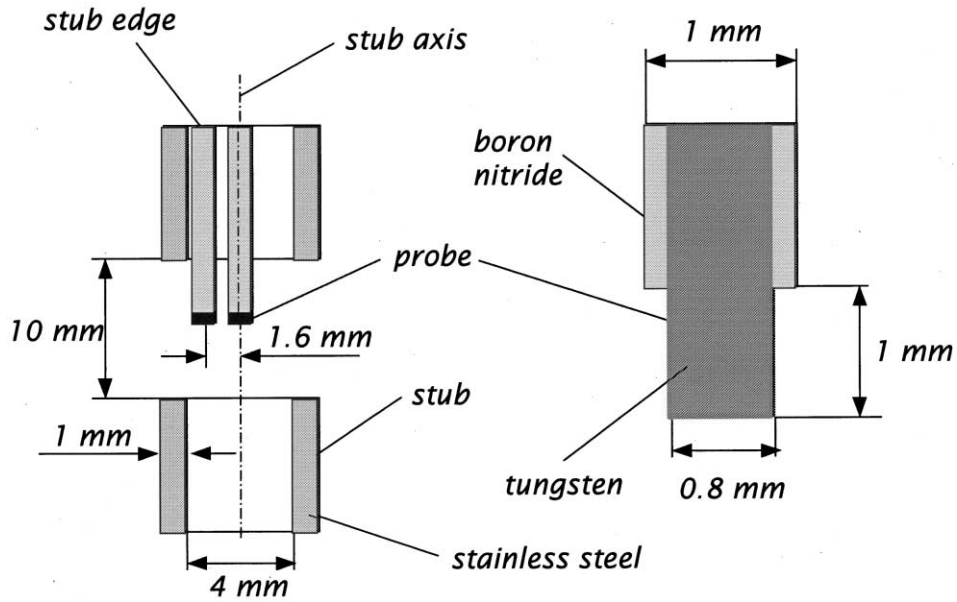


Fig. 7. Probe positions and dimensioning.

particles concentration ( $T = 973$  K) are triplet metastable excited atoms.

Fig. 9 shows two curves collected after 1.7 ms after the discharge ignition under identical discharge conditions, but at two different positions between tubular electrodes. The electron temperature and electron concentration at the axis of the discharge is much lower than at the edge (see corresponding values in Table 4) due to a small penetration depth of the microwaves into very dense plasma and a low mobility of ions at high pressure, not allowing to equalize the ion concentration within few millimeters. Surprising is, that the metastable concentrations calculated from the fitting curves of the negative branches of the probe characteristics do not follow this tendency and are almost equal for both positions.

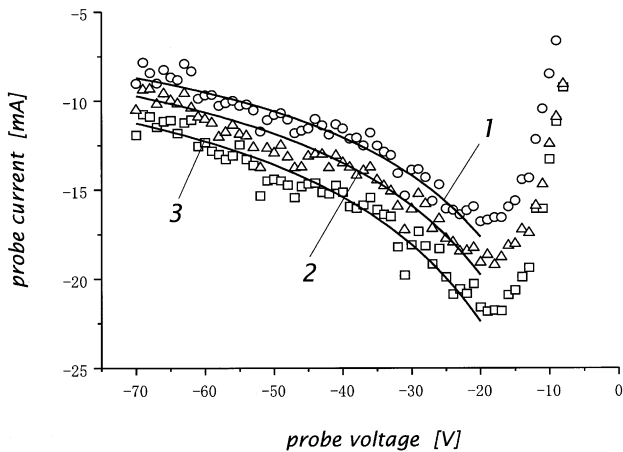


Fig. 8. The negative branches of I–V–probe characteristics measured in 700 Torr helium discharge with three different sets of plasma parameters and emission current fitting curves according to the Eq. (48) and Table 3.

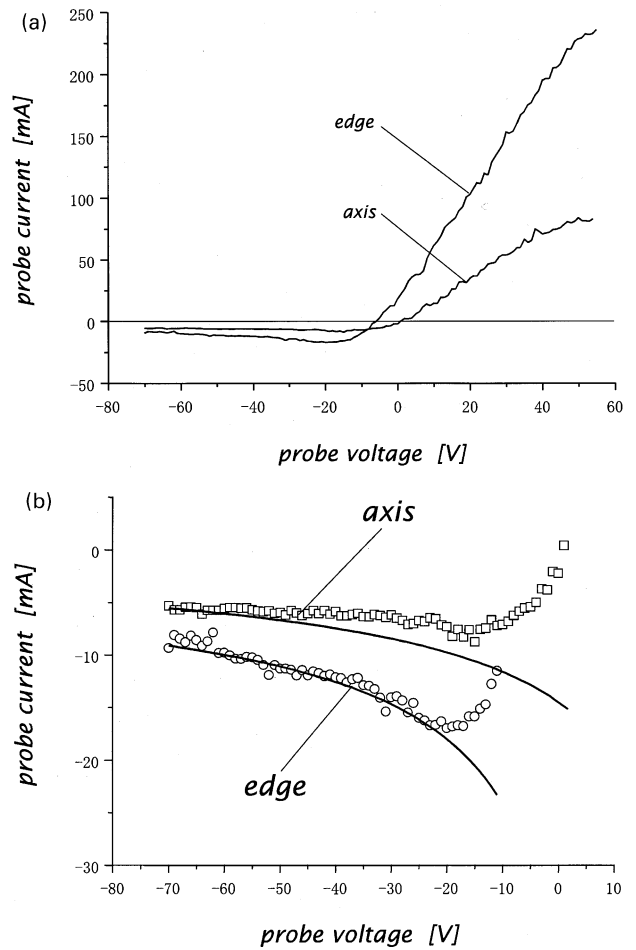


Fig. 9. The probe characteristics collected in 700 Torr helium discharge at 400 W microwave power coupled into plasma at two positions as shown in Fig. 7. (a) The whole curves and (b) the negative branches with fitting curves corresponding the evaluation of metastables concentrations in Table 4.

## 6. Conclusion

For high-density helium discharges at atmospheric pressure, the negative part of the current voltage characteristics can be interpreted as metastables induced secondary emission current. This current is on many orders of magnitude higher, than the collected ion current. The emission current can be described by use of simple analytical expressions. The metastables atom concentration can be estimated from fitting this part of I–V characteristics with modeled curve. The decrease of emission current with increasing negative bias of the probe occurs due to the ion sheath thickness changes. The secondary electron emission current due to metastables de-excitation is decreasing with decreasing pressure.

## Acknowledgements

The authors wish to acknowledge with thanks the work of Takeyama, who took the data published here.

## References

- [1] E.E. Muschlitz, Metastable atoms and molecules, *Science* 159 (1968) 599–604.
- [2] J.S. Chang, et al., Atomic and molecular ionization processes in gases, Tokyo Electric University Press, Tokyo, 1999.
- [3] K.G. Michlewicz, J.J. Urr, J.W. Carnahan, A microwave induced plasma system for the maintenance of moderate power plasmas of helium, argon, nitrogen and air, *Spectrochim. Acta* 40B (1985) 493–499.
- [4] J.-L. Delcroix, C.M. Ferreira, A. Ricard, Metastables atoms and molecules in ionized gases, in: G. Bekefi (Ed.), *Principles of Laser Plasma*, Wiley, New York, 1976.
- [5] G. Sanger, G. Hietkamp, W. Peschka, US Patent 4,631,096.
- [6] L.J. Overzet, J. Kleber, Effect of metastable atom reactions on the electron energy probability functions in afterglows, *Plasma Sources Sci. Technol.* 7 (1998) 512–523.
- [7] K. Tsujii, Y. Yajima, S. Murayama, US Patent 4,615,756.
- [8] M. Kando, Proceedings of Eleventh Symposium Elementary processes and chemical reactions in low temperature plasma, Low Tatras, Slovakia, June 1998, p. 73.
- [9] M. Štefečka, D. Korzec, Y. Imahori, M. Širý, M. Kando, Atmospheric pressure surface discharge: observation of time evolution, *Scitec* 2 (3) (2001).
- [10] F. Massines, G. Gouda, A comparison of polypropylene-surface treatment by filamentary, homogeneous and glow discharges in helium at atmospheric pressure, *J. Phys. D: Appl. Phys.* 31 (1998) 3411–3420.
- [11] Y. Sawada, S. Ogawa, M. Kogoma, Synthesis of plasma-polymerized tetraethoxysilane and hexamethyldisiloxane films prepared by atmospheric pressure glow discharge, *J. Phys. D: Appl. Phys.* 28 (1995) 1661–1669.
- [12] J.Y. Jeong, S.E. Babayan, A. Schütze, V.J. Tu, J. Park, I. Henins, G.S. Selwyn, R.F. Hicks, Etching polyimide with a nonequilibrium atmospheric-pressure plasma jet, *J. Vac. Sci. Technol., A* 17 (1999) 2581–2585.
- [13] H.W. Webb, *Phys. Rev.* 24 (1924) 113.
- [14] M.L.E. Oliphant, *Proc. R. Soc. London* A124 (1929) 228.
- [15] H.D. Hagstrum, The development of ion-neutralization spectroscopy, *J. Vac. Sci. Technol.* 12 (1975) 7–16.
- [16] V.M. Zakharova, Yu.M. Kagan, K.S. Mustafin, V.I. Perel, Probe measurements at medium pressures, *Soviet Phys. Tech Phys.* 5 (1960) 411–418.
- [17] M. Tichý, M. Šicha, P. David, T. David, A collisional model of the positive ion collection by a cylindrical Langmuir probe, *Contrib. Plasma Phys.* 34 (1994) 59–68.
- [18] W.L. Borst, Excitation of metastable argon and helium atoms by electron impact, *Phys. Rev. A* 9 (1974) 1195–1200.
- [19] A.V. Phelps, J.P. Molnar, Lifetimes of metastable states of noble gases, *Phys. Rev.* 89 (1953) 1202–1208.
- [20] A.V. Phelps, Absorption studies of helium metastable atoms and molecules, *Phys. Rev.* 99 (1955) 1307–1313.
- [21] M.A. Biondi, Ionization by the collision of pairs of metastable atoms, *Phys. Rev.* 82 (1951) 453–454.
- [22] S. Klage, M. Tichý, A contribution to the assessment of the influence of collisions on the measurements with langmuir probes in the thick sheath working regime, *Czech. J. Phys. B* 35 (1985) 988–1005.
- [23] Yu.M. Kagan, V.I. Perel, Probes methods in plasma research, *Soviet Phys. Uspekhi* 81 (1964) 767–793.
- [24] I.N. Bronstein, K.A. Semendjajew, G. Musiol, H. Mühlig, *Taschenbuch der Mathematik*, Verlag Harri Deutsch, ISBN 3-8171-2001-X, p. 477.
- [25] W.A. Fitzsimmons, N.F. Lane, G.K. Walters, Diffusion of He( $2^3S_1$ ) in helium gas; ( $2^3S_1$ - $1^1S_0$ ) interaction potentials at long range, *Phys. Rev.* 174 (1968) 193–200.
- [26] R.W. Huggins, J.H. Cahn, Metastable measurements in flowing helium afterglow, *J. Appl. Phys.* 38 (1967) 180–188.
- [27] H.J. Kolker, H.H. Michels, Elastic scattering, diffusion, and excitation transfer of metastable helium in helium, *J. Chem. Phys.* 50 (1969) 1762–1771.
- [28] M.S. Benilov, Can the temperature of electrons in a high-pressure plasma be determined by means of an electrostatic probe?, *J. Phys. D: Appl. Phys.* 33 (2000) 1683–1696.
- [29] I.M. Cohen, Asymptotic theory of spherical electrostatic probes in a slightly ionized, collision-dominated gas, *Phys. Fluids* 10 (1963) 1492–1499.
- [30] H.D. Hagstrum, Theory of Auger ejection of electrons from metal by ions, *Phys. Rev.* 96 (1954) 336–365.
- [31] H.D. Hagstrum, Auger ejection of electrons from tungsten by noble gas ions, *Phys. Rev.* 104 (1956) 317–318.
- [32] V.P. Nagorny, P.J. Drallos, Effective secondary emission coefficient in a high-pressure noble gas, *Plasma Sources Sci. Technol.* 6 (1997) 212–219.
- [33] H.D. Hagstrum, Auger ejection of electrons from tungsten by noble gas ions, *Phys. Rev.* 96 (1954) 325–335.
- [34] D.E. Golden, H.W. Bandel, Absolute total electron-helium-atom scattering cross sections for low electron energies, *Phys. Rev.* 138 (1965) A14–A21.
- [35] D.A. MacLennan, Electron ejection from an atomically clean tungsten surface by Helium and Neon metastable atoms, *Phys. Rev.* 148 (1966) 218–223.
- [36] M.R. Telukder, D. Korzec, M. Kando, Probe diagnostics in high pressure high density microwave discharge, *Plasma Science Symposium 2001/The 18th Symposium on Plasma Processing (PSS-2001/SPP-18)*, January 24–26, Kyoto, Japan, 2001.